Article

Current Biology

ACA pumps maintain leaf excitability during herbivore onslaught

Highlights

- The defenses of an *Arabidopsis* Ca^{2+} pump mutant fail when attacked by insects
- This correlates with loss of ability to propagate electrical signals in leaves
- Electrical signaling can be restored by expressing a Ca^{2+} pump gene in veins
- Ca^{2+} pump action prevents senescence during prolonged or repetitive stress

Authors

Nikou Fotouhi, Michaela Fischer-Stettler, Gioia Lenzoni, Stéphanie Stolz, Gaëtan Glauser, Samuel C. Zeeman, Edward E. Farmer

Correspondence

edward.farmer@unil.ch

In brief

Insect-attacked leaves produce electrical signals. Fotouhi et al. identify an *Arabidopsis* mutant that loses its ability to produce electrical signals when damaged by insects. The plant's normally robust defense system fails, and it undergoes senescence. The work identifies genes that maintain plant membrane excitability under prolonged stress.

Fotouhi et al., 2022, Current Biology *32*, 2517–2528
June 6, 2022
https://doi.org/10.1016/j.cub.2022.03.059

CellPress

Current Biology

CellPress
OPEN ACCESS

Article

ACA pumps maintain leaf excitability during herbivore onslaught

Nikou Fotouhi,[1] Michaela Fischer-Stettler,[2] Gioia Lenzoni,[1] Stéphanie Stolz,[1] Gaëtan Glauser,[3] Samuel C. Zeeman,[2] and Edward E. Farmer[1,4,*]

[1]Department of Plant Molecular Biology, University of Lausanne, 1015 Lausanne, Switzerland
[2]Institute of Molecular Plant Biology, ETH Zürich, Universitätstrasse 2, 8092 Zürich, Switzerland
[3]Neuchâtel Platform of Analytical Chemistry, University of Neuchâtel, 2000 Neuchâtel, Switzerland
[4]Lead contact
*Correspondence: edward.farmer@unil.ch
https://doi.org/10.1016/j.cub.2022.03.059

SUMMARY

Recurrent damage by lepidopteran folivores triggers repeated leaf-to-leaf electrical signaling. We found that the ability to propagate electrical signals—called slow wave potentials—was unexpectedly robust and was maintained in plants that had experienced severe damage. We sought genes that maintain tissue excitability during group insect attack. When *Arabidopsis thaliana* P-Type II Ca^{2+}-ATPase mutants were mechanically wounded, all mutants tested displayed leaf-to-leaf electrical signals. However, when the auto-inhibited Ca^{2+}-ATPase double-mutant *aca10 aca12* was attacked by *Spodoptera littoralis* caterpillars, electrical signaling failed catastrophically, and the insects consumed these plants rapidly. The attacked double mutant displayed petiole base deformation and chlorosis, which spread acropetally into laminas and led to senescence. A phloem-feeding aphid recapitulated these effects, implicating the vasculature in electrical signaling failure. Consistent with this, *ACA10* expressed in phloem companion cells in an *aca10 aca12* background rescued electrical signaling and defense during protracted *S. littoralis* attack. When expressed in xylem contact cells, *ACA10* partially rescued these phenotypes. Extending our analyses, we found that prolonged darkness also caused wound-response electrical signaling failure in *aca10 aca12* mutants. Our results lead to a model in which the plant vasculature acts as a capacitor that discharges temporarily when leaves are subjected to energy-depleting stresses. Under these conditions, ACA10 and ACA12 function allows the restoration of vein cell membrane potentials. In the absence of these gene functions, vascular cell excitability can no longer be restored efficiently. Additionally, this work demonstrates that non-invasive electrophysiology is a powerful tool for probing early events underlying senescence.

INTRODUCTION

Herbivore attack is a high-intensity stress that plants in nature encounter frequently. Moreover, innumerable insect species lay their eggs in clutches so that large numbers of neonates begin their lives attacking individual leaves and shoots.[1] This behavior is exemplified by the generalist lepidopteran *Spodoptera littoralis*. Other herbivores such as the aphid *Brevicoryne brassicae* congregate and reproduce as colonies on leaf blades, petioles, and stems. These group-feeding strategies may confer benefits to the attackers, such as the improvement of food quality.[2] The pressure that invertebrate herbivores can exert on plant physiology is considerable. For example, entire plants can be consumed by insects such as locusts. In many cases when plants are not destroyed, insect attack triggers senescence in the host plant. This is the case, for example, when Arabidopsis is attacked by the aphid *Myzus persicae*.[3] However, we are unaware of reports of senescence in Arabidopsis caused by chewing herbivores.

Chewing insects elicit reiterated energy-consuming responses in the plant. For example, feeding caterpillars trigger repeated bursts of electrical activity in leaves.[4–6] Low levels of damage, such as bites to the edges of Arabidopsis leaf blades, provoke repetitive high-amplitude (>40 mV) membrane depolarization events that spread from the lamina to petioles in the damaged leaves (e.g., Video S1[5]). More severe herbivore-inflicted damage to midveins or petioles triggers longer-duration leaf-to-leaf electrical signals called slow wave potentials (SWPs; Video S1[7]). These electrical activities trigger the synthesis of jasmonates, including the defense mediator jasmonoyl-isoleucine (JA-Ile), and contribute to defense against the chewing herbivore *S. littoralis*.[5,8] Moreover, other signaling events are coupled to membrane depolarization. For example, wound-response electrical signals are genetically linked to cytosolic Ca^{2+} increases[8] that may regulate defense gene expression.[9–11] As with damage-response electrical signals, cytosolic Ca^{2+} transients in Arabidopsis are more rapid and more intense in primary veins in petioles than elsewhere in the leaf.[7,8] Even though the herbivore-induced accumulation of defense proteins and chemicals helps to ensure plant survival, it is potentially costly.[12] That is, multiple drains on chemical energy may be incurred to maintain leaf function during attack. For example,

membrane potentials have to be restored repeatedly after bite damage. Although many plant defense genes are known,[13] those that act to maintain the physiological functions of leaves and petioles during sustained herbivore onslaught remain poorly characterized. During the attack process, the products of such genes might function in cellular ion and proton homeostasis and/or in the restoration of energy balance in critical cell populations.

During an investigation of electrical signaling in Arabidopsis, we noticed that leaf-to-leaf SWPs occurred even in plants that had been severely damaged by insects over the course of several days. Such a sustained and robust electrical signaling response was unexpected. We therefore investigated genetic mechanisms that underpin electrical signaling in insect-damaged plants. To do so, we sought mutants that disrupt the propagation of leaf-to-leaf SWP signals. Since cytosolic Ca^{2+} transients and damage-induced electrical signals are coupled genetically,[8] we reasoned that mutations affecting Ca^{2+} homeostasis might interfere with the plant's leaf-to-leaf electrical signaling capacity. As candidate genes for a reverse genetic screen we chose a 14-member subfamily of P-type II Ca^{2+}-ATPases in *Arabidopsis*. These Ca^{2+}-ATPases,[14–15] which are part of a much larger Ca^{2+} transport and signaling machinery,[16,17] fall into two clades: type IIA (ER-type Ca^{2+}-ATPases; ECAs) and type IIB (auto-inhibited Ca^{2+}-ATPases [ACAs]). Mutations in *ACA* genes can cause spontaneous lesions on leaves,[18,19] affect defense,[20,21] and perturb cytosolic Ca^{2+} homeostasis.[19,22,23] Moreover, the mutation of type II Ca^{2+}-ATPases can have broader effects on plant growth and function.[21] Each of these considerations made P-type II Ca^{2+}-ATPase genes attractive targets that, when mutated, might perturb electrical signaling in petioles.

Using non-invasive surface electrodes placed near petiole bases, we initially screened a library of P-type II Ca^{2+} ATPase single and double mutants for electrical signal characteristics following an acute mechanical wound. This screen failed to reveal any mutants that impacted electrical signal propagation. However, when the same mutant library was re-screened using quantitative herbivory bioassays, an *aca* double mutant with high susceptibility to *S. littoralis* was identified. The re-analysis of electrical signaling in those plants, following chronic insect damage, yielded unexpected results.

RESULTS

Robust leaf-to-leaf electrical signaling in the insect-damaged wild type

Wild-type (WT) plants grown in short-day conditions for 5 weeks were caged for 9 days in the absence or presence of 8 neonate *S. littoralis* caterpillars per plant (STAR Methods). The control plants on which no larvae were placed displayed no leaf damage (Figure 1A) or petiole reddening (Figure 1B). To test electrical signaling capacity, a surface electrode was placed on the petiole of leaf 13 at a distance of 1 cm from the rosette center (Figure 1C). A reference electrode was placed in the soil.[8] Leaf 8 was wounded mechanically by crushing the apical 60% of the lamina as shown in Figure 1C. These plants produced SWPs (Figure 1D), which were quantified (Figure 1E) as reported previously.[5] Plants on which *S. littoralis* had fed for 9 days showed damage to expanded leaves (Figure 1F) and reddening of the basal adaxial petiole surfaces of expanded leaves (Figure 1G). When these plants were wounded mechanically (Figure 1H), they produced SWPs with architectures (Figure 1I), amplitudes, and durations (Figure 1J) similar to those of the undamaged plants. We noted, however, that the latency, i.e., the time taken from wounding leaf 8 until the electrical signal reached the petiolar electrode on leaf 13, was 50.7 ± 8.4 s (standard deviation; n = 7) in the previously undamaged WT and 95.8 ± 2.7 s in the damaged WT upon which larvae had fed for 9 days.

Ca^{2+} pump mutants failed to strongly affect electrical signaling after mechanical wounding

Since wound-response electrical signaling and cytosolic Ca^{2+} transients in leaves are linked genetically,[8] we assumed that interference with Ca^{2+} homeostasis might affect electrical signaling. A collection of 23 *aca* and *eca* single and double T-DNA insertion mutants was generated to test this hypothesis. The mutants (Figure S1; Table S1) were grown in soil under short-day conditions and screened in the adult phase for SWP responses. To do this, leaf 8 was wounded with forceps, and the amplitudes and durations of SWPs were monitored on distal leaf 13 as shown in Figure 1C. None of the mutants significantly affected the SWP (Table S1). We then decided to re-screen the mutant collection for defense capacity when challenged with *S. littoralis* caterpillars.

The *aca10 aca12* mutant is hypersusceptible to *S. littoralis*

Using no-choice bioassays with neonate *S. littoralis*, we compared larval weight gain 11–14 days after the initiation of feeding on the *aca* and *eca* mutant collection. In these experiments, the *aca10 aca12* double mutant stood out as being extremely susceptible to *S. littoralis* relative to the WT (Table S2). Additional experiments confirmed that *S. littoralis* larvae gained weight less rapidly on the WT than on *aca10 aca12* double mutants (Figure 2A). At the end of bioassays, the leaves of the WT plants were still green, but many of the expanded leaves of the insect-damaged *aca10 aca12* double mutant had yellowed (Figure 2B). We noted that prior to severe chlorosis of the entire laminas of the double mutant, apparent signs of stress were visible on the petioles of some leaves. After allowing *S. littoralis* to feed for 3.5 days, we observed no deformation or chlorosis on the petioles of the WT (Figure 2C), even in cases where the petiole had been bitten (Figure 2D). However, in the *S. littoralis*-damaged *aca10 aca12* plants at this time point, we noticed translucency and apparent shrinkage of small regions of some petioles (Figure 2E). This was not associated with direct feeding damage to these petioles.

Generation of the *aca10c aca12c* CRISPR-Cas9 mutant

To confirm that our observation of extreme susceptibility to *S. littoralis* could be recapitulated in an independent genetic background, we generated an *aca10c aca12c* double mutant using CRISPR-Cas9 mutagenesis (Figure S2A). Consistent with a previous report,[21] when grown in constant light, the inflorescence stems of the flowering-phase *aca10 aca12* T-DNA insertion mutant and the CRISPR-Cas9-generated *aca10c aca12c* plants were shorter than those of the WT (Figure S2B). However,

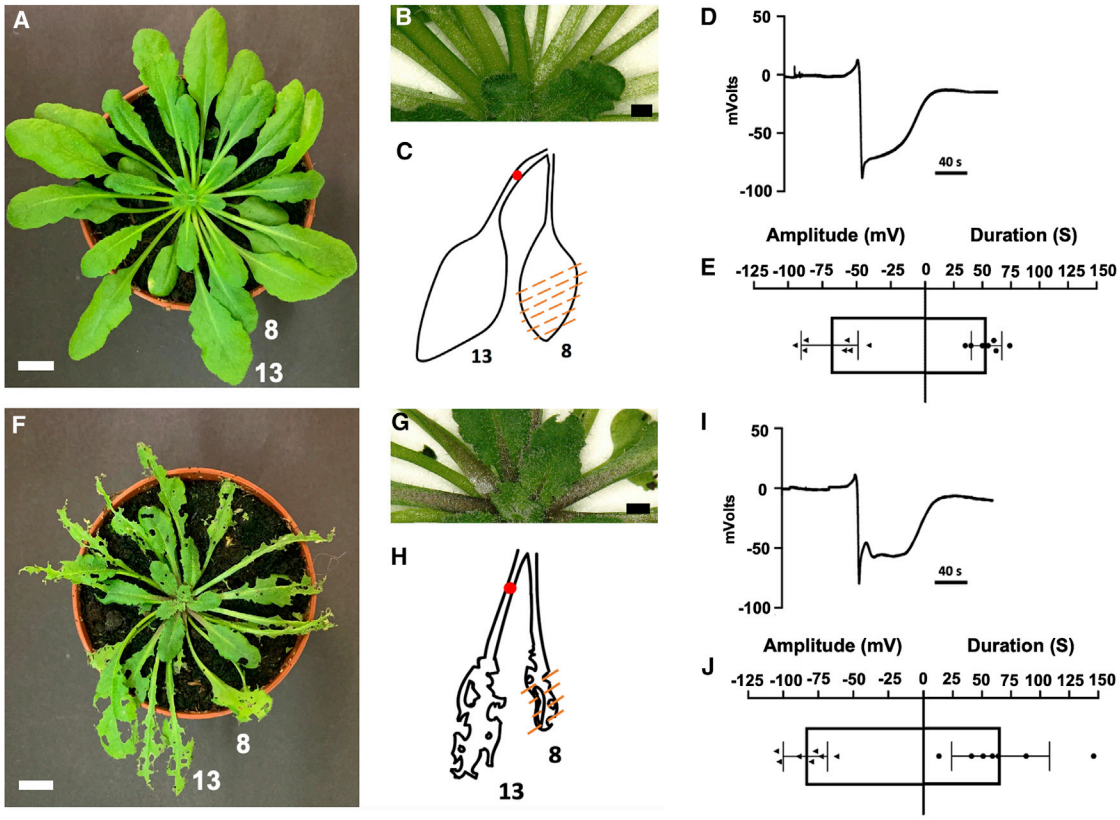

Figure 1. Leaf-to-leaf electrical signaling in caterpillar-damaged wild-type plants

(A) 5-week-old plants were caged in the absence of insects for 9 days. Leaves 8 and 13 are indicated.

(B) Detail of petioles near the rosette center.

(C) Strategy for mechanical wounding of leaf 8 and recording electrical activity on leaf 13. An electrode (red dot) was placed on the leaf 13 petiole 1 cm from the rosette center.

(D) A representative recording from the petiole of leaf 13 after mechanically crush wounding (orange hatching) leaf 8 of an undamaged WT plant.

(E) Electrical signal duration and amplitude in previously undamaged WT plants.

(F) Plants caged with *S. littoralis* neonate larvae (8 per plant) for 9 days. Leaves 8 and 13 are indicated.

(G) Detail of petioles near the rosette center. Note basipetal petiole reddening.

(H) Strategy for mechanical wounding of leaf 8 and recording electrical activity on leaf 13.

(I) Representative recording from leaf 13 petiole after crush wounding leaf 8 of a *Spodoptera*-damaged WT plant.

(J) Electrical signal duration and amplitude in *Spodoptera*-damaged WT plants.

For (E) and (J), data are shown as means ± SD (7 biological replicates). Scale bars, 1 cm in (A) and (F). Scale bars, 1 mm in (B) and (G).

See also Table S1.

in the short-day-grown adult phase, and in the total absence of insects, the *aca10c aca12c* double mutant showed a rosette phenotype similar to that of both the *aca10 aca12* T-DNA insertion mutant and the WT (Figure S2C). When challenged with *S. littoralis*, both the T-DNA insertion *aca10 aca12* mutant and the *aca10c aca12c* CRISPR-Cas9 mutant displayed more feeding damage to leaves than did the WT (Figure S2C).

Cytosolic Ca^{2+} in wounded *aca* double mutants

To investigate whether wound-response Ca^{2+} levels were affected in *aca10c aca12c*, this plant was crossed with an *UBQ10*$_{pro}$*:GCaMP3* intensometric calcium reporter line.[8] Expression of genetically encoded calcium reporters can inhibit plant growth.[24] We found that homozygous *aca10c aca12c* harboring *UBIQUITIN10*$_{pro}$*:GCaMP3* showed severely stunted growth that precluded their use in experiments. We therefore crossed *aca10c aca12c* with a WT background expressing the ratiometric Ca^{2+} reporter yellow cameleon 3.6 (YC3.6) driven by the *UBQ10* promoter.[25] Double-mutant plants harboring this transgene had phenotypes similar to the WT. The mechanically wounded *aca10c aca12c* double mutant produced cytosolic Ca^{2+} transients with similar architectures but with lower amplitudes to those in the WT (Figures S2D and S2E). The FRET/CFP ratios of the reporter, both prior to and after wounding, were lower in the *aca10c aca12c* background than in the WT (Figures S2F–S2I).

aca10 aca12 leaves fail to propagate SWPs after chronic insect attack

Next, we attempted to elicit leaf-to-leaf electrical signaling in *Spodoptera*-damaged plants. *S. littoralis* neonates were allowed to feed for 3.5 days, and then leaf-to-leaf electrical signaling was

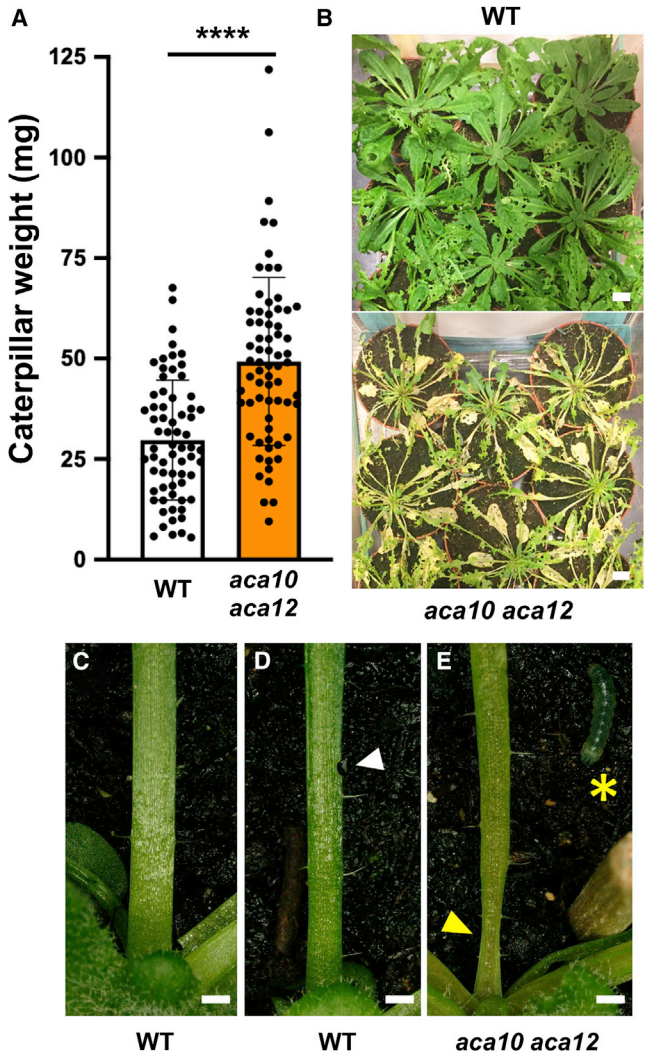

Figure 2. *Spodoptera littoralis* performance and feeding damage on *aca10 aca12* versus WT

(A) Insect weight gain on the WT and *aca10 aca12*. Neonate *S. littoralis* larvae (4 per plant) were placed on each of the 22 plants. Insects were allowed to feed continuously under short-day conditions. Surviving larvae were weighed individually after 12 days feeding. Means ± SD (Student t test, ****$p < 0.0001$).

(B) WT and *aca10 aca12* rosettes at the end of the 12-day feeding period. (A) and (B) are from different experiments. Scale bars, 1 cm.

(C) Basal petiole from an *S. littoralis*-damaged WT plant.

(D) Bite damage to WT petioles did not cause petiole deformation.

(E) Basal petiole deformation in an *S. littoralis*-attacked *aca10 aca12* double mutant. The petioles photographed were from leaves 7–14. Note petiole deformation (yellow arrowhead) and larva (yellow asterisk). For (C)–(E), 8 *S. littoralis* neonates were placed on 5.5-week-old plants and allowed to feed for 3.5 days. Scale bars, 1 mm.

See also Table S2 and Figure S1.

monitored on the leaf 13 petiole after mechanically wounding leaf 8. As expected, the *Spodoptera*-damaged WT successfully produced SWPs. Remarkably, *aca10c aca12c* plants on which *S. littoralis* had fed only rarely transmitted SWPs to the distal leaf 13 (Figure 3A). A time course experiment using *S. littoralis* revealed that both the amplitudes and durations of SWPs decreased in parallel in *aca10c aca12c* during attack by *S. littoralis* (Figure 3B). In the WT, the amplitude of the SWP was maintained over the entire experiment although the duration of the SWP was shortened midway through the time course. As expected, the weights of *aca10c aca12c* rosettes diminished more rapidly than those of the WT (Figure 3C). In parallel, tissue loss was more extensive in the double mutant than in the WT (Figure 3D). Leaves 6–10 of *aca10c aca12c* were inspected for signs of petiole shrinkage during a *Spodoptera*-feeding time course experiment (Figure 3E). Petioles displaying shrinkage were detected from day 3 onward in the double mutant (Figure 3F), although at this time point only 3 of 6 plants showed petiole shrinkage affecting a single leaf on each plant. No areas of shrunken petiole were detected in undamaged control plants or in the insect-damaged WT.

To test whether the effects of *Spodoptera* feeding on electrical signaling were insect-specific, we examined the plant's response to a herbivore from a different insect order. Cabbage aphids (*Brevicoryne brassicae*), which pierce rather than chew plant tissues and which, unlike *Spodoptera*, selectively target the phloem,[26] were allowed to feed for 7 days on WT and *aca10c aca12c* plants. At that point, leaf 8 of WT and *aca10c aca12c* plants was wounded mechanically and electrical signals were monitored on distal leaf 13. Both the uninfested WT and the uninfested *aca* double mutant produced strong leaf-to-leaf electrical signals. However, we found a striking failure of aphid-infested double mutants to propagate wound-response electrical signals from leaf to leaf (Figure S3A). The basal petioles of expanded leaves of the *Brevicoryne*-infested mutant plants frequently appeared translucent and were sometimes deformed, whereas those of the control (uninfested) double mutant and the WT did not display these features (Figure S3B). We noted that *B. brassicae* aphids caused strong growth arrest in *aca10 aca12* (Figure S3C) and that chlorophyll levels were lower in the *B. brassicae*-attacked double mutant than in the attacked WT (Figure S3D).

Biochemical characterization of *aca10 aca12* double mutants

Senescing plants display chlorophyll breakdown that reduces photosynthesis, and they typically initiate chloroplast degradation, which can remobilize sugars and membrane lipids, and release free amino acids from proteins.[27] The chlorotic features of insect-attacked *aca10 aca12* double mutants suggested that they were undergoing a form of senescence. Chlorophyll levels were measured and found to be lower in the leaves of the *Spodoptera*-attacked *aca10c aca12c* double mutant than in the attacked WT (Figure 4A). Sugar analyses revealed that fructose levels were increased in the *Spodoptera*-damaged *aca10c aca12c* mutant compared with the damaged WT (Figure 4B). There were also significant changes in free amino acids, as the levels of 10 canonical amino acids (Arg, Asn, Asp, Cys, Gln, His, Ile, Leu, Phe, and Trp) were significantly higher in the *Spodoptera*-attacked double mutant than in the attacked WT (Figure 4C).

Levels of several glucosinolates were found to be higher in the undamaged WT than in the undamaged *aca* double mutant. However, 4-methoxyindol-3-yl methyl glucosinolate (4MOI3M) was present at higher levels in undamaged *aca10 aca12* than in the WT (Figures S4A–S4H). With the exception of 4MOI3M, glucosinolate levels were generally higher in the *S. littoralis*-attacked WT than in the double mutant. Next, JA-Ile levels were compared

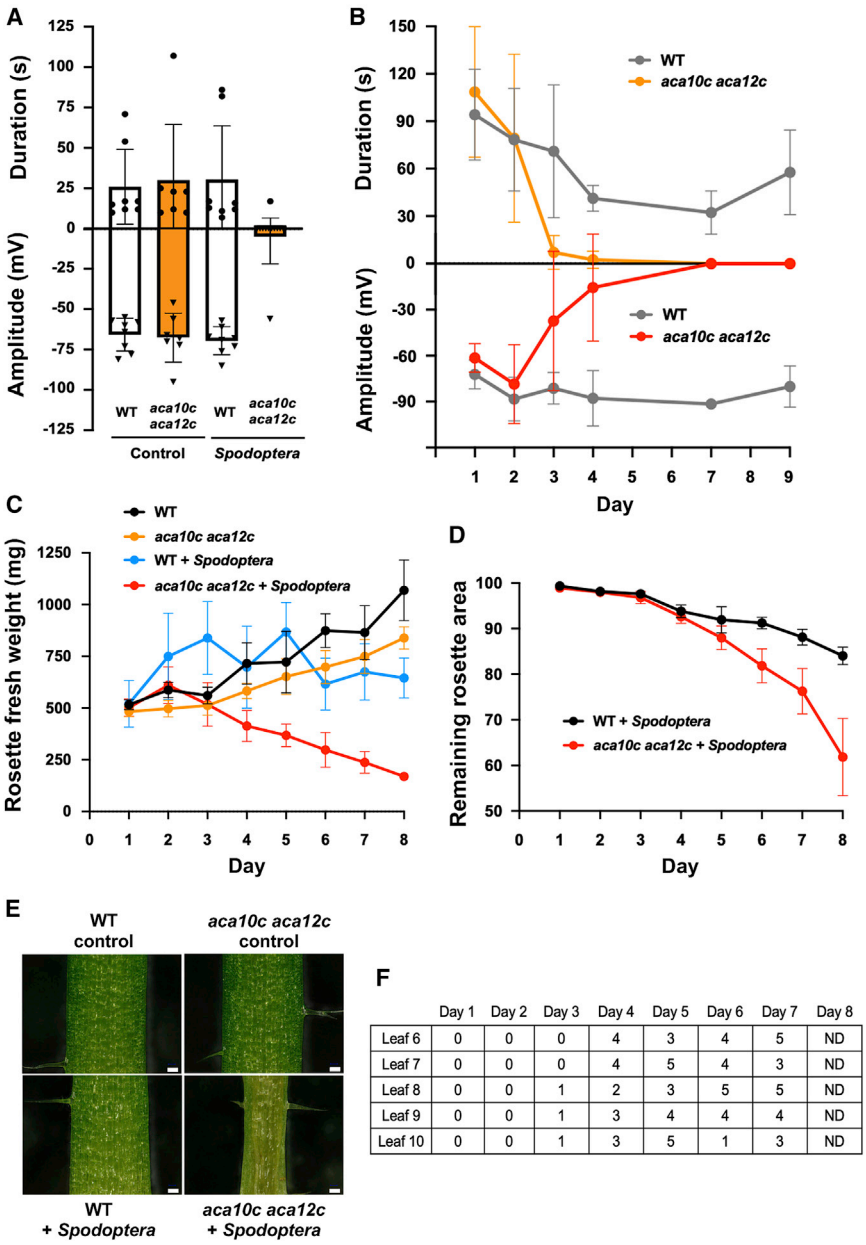

F

	Day 1	Day 2	Day 3	Day 4	Day 5	Day 6	Day 7	Day 8
Leaf 6	0	0	0	4	3	4	5	ND
Leaf 7	0	0	0	4	5	4	3	ND
Leaf 8	0	0	1	2	3	5	5	ND
Leaf 9	0	0	1	3	4	4	4	ND
Leaf 10	0	0	1	3	5	1	3	ND

Figure 3. Electrical signaling failure, mass loss, and petiole deformation in *Spodoptera*-attacked plants

(A) Leaf-to-leaf electrical signaling failure in *S. littoralis*-attacked *aca10c aca12c*. Neonate larvae (8 per plant) were allowed to feed for 3.5 days. Control plants were caged without insects. Electrical signals were monitored on the petiole of leaf 13 after mechanically crush wounding leaf 8. Data are means ± SD (n = 7–8 biological replicates).

(B) Time course for the effect of *S. littoralis* feeding on surface potentials. At each time point an insect-damaged expanded leaf (leaf 8–11) was crush-wounded, and surface potentials were measured on leaf n + 5 (i.e., a leaf sharing a direct vascular connection with the wounded leaf). Data shown are means ± SD (n = 4–9).

(C) Rosette fresh weights during *S. littoralis* feeding on the WT and *aca10c aca12c* double mutant. Error bars show means ± SD (n = 6 rosettes).

(D) Estimated plant tissue loss (%) due to *S. littoralis* feeding. Data are presented as the ratios of remaining lamina surface divided by total estimated leaf surface. Error bars show means ± SD (n = 6 rosettes). For (B), (C), and (D), neonates (4 per plant) were placed on 5-week-old rosettes.

(E) Detail of basal petiole phenotypes in control or *S. littoralis*-infested plants used for electrophysiology. Scale bars, 0.1 mm. 5.5-week-old plants were caged with or without 8 neonate *S. littoralis* larvae for 3.5 days.

(F) Petiole shrinkage measured on leaves 6–10 of *S. littoralis*-attacked *aca10c aca12c* plants. Data from 6 plants with 4 larvae at each time point. See STAR Methods for details of scoring petioles. ND, not distinguishable due to severe damage of leaves, which made leaf number assignment ambiguous.

See also Figures S2 and S3.

in the leaves of undamaged plants and in plants on which *S. littoralis* neonates were allowed to feed. In insect-damaged plants, JA-Ile (Figure S4I) levels were higher in the double mutant than in the WT. Additionally, JA-Ile levels were assessed in the WT and in *aca10 aca12* after single crush wounds. In these experiments, the levels of JA-Ile were similar in both genotypes (Figure S4J). Levels of transcripts for the jasmonate-responsive gene *VEGETATIVE STORAGE PROTEIN 2* (*VSP2*) were assessed after *S. littoralis* feeding. These transcript levels were similar in the insect-damaged WT and *aca10 aca12* plants (Figure S4K).

Tissue-specific complementation

Are there specific cell populations in *aca10 aca12* mutants that might be responsible for the extreme susceptibility to herbivores and failure to transmit SWPs? To address this, we attempted to complement the *aca10c aca12c* double mutant with a genomic *ACA10* clone fused to β-glucuronidase (GUS) expressed under tissue-specific promoters. SWP transmission is known to require both the xylem and the phloem.[8] The *LIPOXYGENASE 6* (*LOX6*) promoter[28] was used to express *ACA10-GUS* in xylem contact cells, and the *SUCROSE TRANSPORTER 2* (*SUC2*) promoter[29] was used to express *ACA10* in phloem companion cells. Additionally, *ACA10-GUS* was expressed under the control of the *CHLOROPHYLL a/b BINDING PROTEIN 3* (*CAB3*) promoter, which is expressed in many cell types, including the mesophyll[30] and phloem companion cells.[31] Using the *aca10c aca12c* mutant as a control, three individual T2 generation plants per transformation were screened for susceptibility to *S. littoralis*. From these plants, representative lines were then assessed for GUS activity in extracted veins (Figure S5A) and in transversal petiole sections (Figure S5B). GUS staining in $SUC2_{pro}$:*ACA10-GUS* and

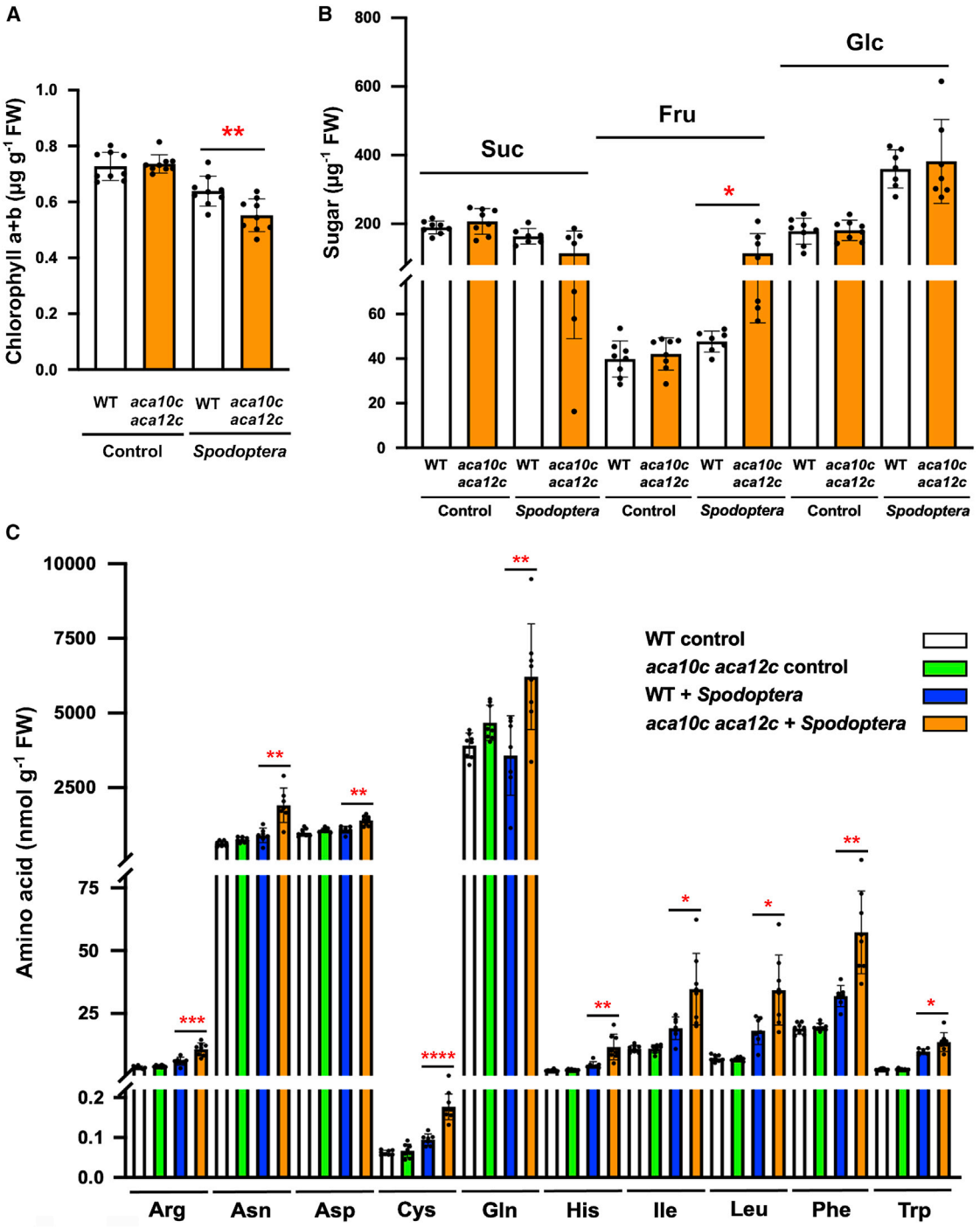

Figure 4. Chlorophyll, sugar, and amino acid levels after insect attack

S. littoralis (8 neonates per plant) were placed on 5.5-week-old WT and *aca10c aca12c* plants in short-day conditions. Leaves were harvested after 3.5 days. Control plants were incubated identically in the absence of insects.

(A) Chlorophyll levels (n = 9 biological replicates).

(B) Sugar levels (n = 7–8 biological replicates).

(C) Amino acid levels (n = 7–8 biological replicates). Data shown are means ± SD, (Student t test, *p < 0.05, **p < 0.01, ***p < 0.001, ****p < 0.0001).

See also Figure S4.

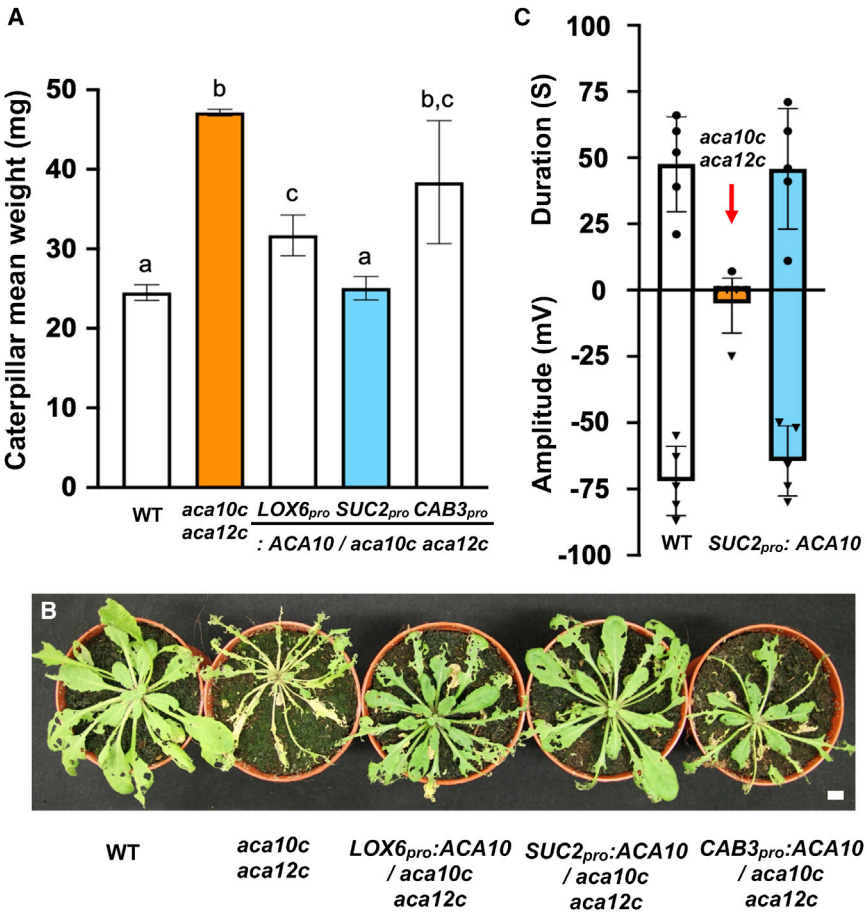

Figure 5. Tissue-specific expression of *ACA10* in the *aca10c aca12c* background

Translational *ACA10*-GUS fusions were expressed under the *LOX6*, *SUC2*, or *CAB3* promoters in *aca10c aca12c*. *S. littoralis* larvae (4 neonates per plant) were placed on 5.5-week-old T2 generation complemented lines and allowed to feed for 10 days.

(A) Caterpillar masses at the end of the feeding period. The results are from two combined assays each using 11 plants. Letters indicate significance differences in a Tukey HSD test ($p < 0.01$). The significance of the difference between weight gain on *aca10c aca12c* and $CAB3_{pro}$*:ACA10-GUS/ aca10c aca12c* was $p = 0.2507$ (Student t test).

(B) Representative rosettes at 10 days after insect feeding. Scale bars, 1 cm.

(C) Electrical signaling in WT, *aca10c aca12c* and $SUC2_{pro}$-complemented *aca10c aca12c* plants 10 days after onset of *S. littoralis* feeding.

See also Figure S5.

$LOX6_{pro}$*:ACA10-GUS* was intense in the phloem and xylem regions, respectively. Although easily detectable in isolated veins, $CAB3_{pro}$*:ACA10-GUS* staining in transversal sections was weak and widespread, extending to non-vascular tissues.

We allowed neonate *S. littoralis* larvae to test the defenses of these transformants. After allowing insects to feed for 10 days, plants were assessed for insect damage. In these assays, insects grown on the $LOX6_{pro}$*:ACA10-GUS* plants gained more weight than they did on the WT, but less than on the double mutant. Larval weight gain on $SUC2_{pro}$*:ACA10-GUS*-expressing mutants was similar to that on the WT (Figure 5A), and the $SUC2_{pro}$*:ACA10-GUS* plants showed near WT signs of leaf damage. The $LOX6_{pro}$*:ACA10-GUS* plants displayed intermediate levels of leaf damage, and there was extensive damage to expanded leaves of the *aca10c aca12c* double mutant with or without $CAB3_{pro}$*:ACA10-GUS*. Nevertheless, the youngest leaves of the $CAB3_{pro}$*:ACA10-GUS* plants displayed less damage than those of the double mutant without the transgene (Figure 5B). Given the pronounced effects of *ACA10* rescue in the phloem on insect weight gain, SWP signaling in these lines was compared with that of the WT and the double mutant. After a 10-day feeding period, the SUC2 promoter-driven *ACA10-GUS* / *aca10c aca12c* plants showed robust WT-like electrical signals (Figure 5C).

Prolonged darkness triggers senescence in *aca10 aca12*

Prolonged darkness can cause senescence in plants.[32] We did not observe darkness-induced senescence in the WT or in the *aca10* and *aca12* single mutants after incubation in continuous darkness for 3 days (Figures 6A and 6B). All three genotypes produced SWPs after exposure to darkness (Figure 6C). Similar experiments were then conducted with the *aca10 aca12* double mutants. After 3 days of darkness, both the T-DNA insertion- and the CRISPR-generated *aca10 aca12* double mutants had begun to display chlorosis and wilting whereas the WT did not (Figure 6D). We noted that darkness-induced senescence in the double mutants differed in several ways to the insect-damage-induced senescence-like phenotypes. Basal petiole deformation as observed in the *S. littoralis*-attacked double mutants was not observed in dark-treated double mutants. However, the double mutants maintained in darkness for 3 days often displayed waterlogging symptoms in leaf blades (Figure 6E). We then examined electrical signaling in the *aca10c aca12c* double mutants. Since these plants already showed signs of senescence after 3 days of darkness, a shorter (24 h) incubation in the dark was tested. Whereas SWP generation was maintained in the 24 h-dark-treated WT, it failed completely in the *aca10c aca12c* double mutant, even though visible signs of chlorosis were absent in both genotypes (Figure 6F).

DISCUSSION

We found that leaf-to-leaf electrical signaling in the WT was unexpectedly robust, occurring between leaves that had been badly damaged by herbivores. Similarly, WT plants that had been placed in total darkness for 3 days were still able to propagate SWPs. Intriguingly, by screening a collection of *eca* and *aca* mutants, we found a double mutant that, despite showing

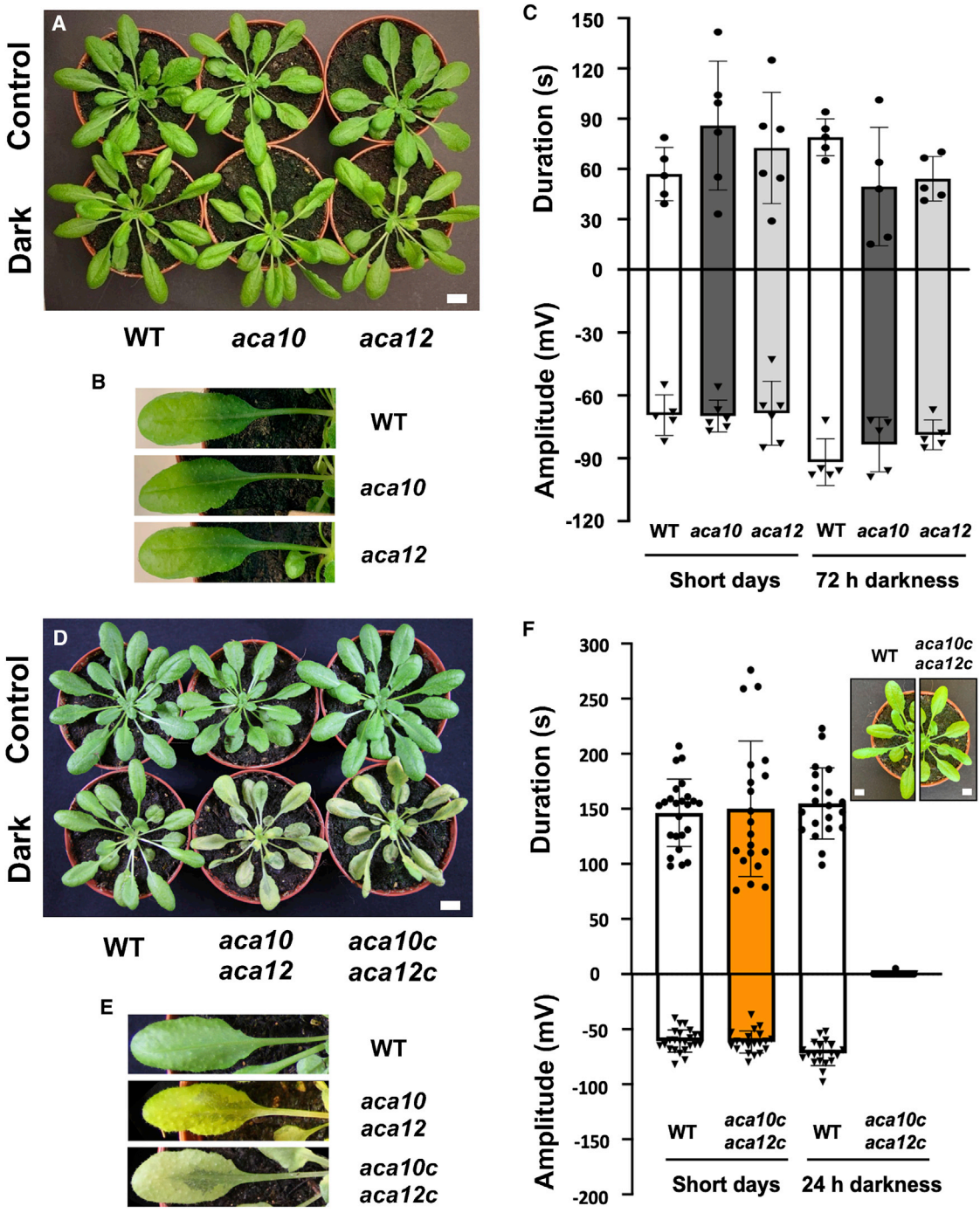

Figure 6. Effects of prolonged darkness on electrical signaling in *aca* mutants

(A) Phenotypes of the WT and the *aca10* and *aca12* single-mutant rosettes in short-day conditions (upper row) or after 3 days darkness (lower row). 5-week-old plants were transferred to darkness at 12h00 (ZT = 4 h) and left in darkness for 72 h. Scale bars, 1 cm.

(B) Leaf and petiole appearance after 3 days darkness.

(C) SWPs in the dark-treated WT and *aca* single mutants. After 3 days dark treatment, plants were transferred back to light and SWPs were measured within 1 h on leaf 13, following single mechanical wounds on leaf 8. Means ± SD, n = 5–6.

(D) Phenotype of the WT, T-DNA insertion mutant *aca10 aca12*, and the CRISPR-Cas9-generated *aca10c aca12c* rosettes after culture in short-day conditions (upper row) or after 3 days continuous dark treatment (lower row). Scale bars, 1 cm.

(E) Waterlogging in dark-treated *aca* double-mutant leaves. The WT, *aca10 aca12*, and *aca10c aca12c* plants were photographed after 3 days in darkness. Note chlorosis and waterlogging (dark patches) in leaves of the mutants.

(legend continued on next page)

WT-like SWPs in response to a single mechanical wound, failed catastrophically to transmit leaf-to-leaf electrical signals after it had suffered prolonged insect damage. These findings underscore the shortcomings of using acute mechanical wounds as a substitute for studying the effects of insect attack on plants. In nature, and in a fascinating parallel to necrotrophic pathogens, many insect herbivores activate senescence processes in their host plants. These "senescence-feeders" form a large guild that includes members from both Lepidoptera and Hemiptera.[33] Indeed, the aphid *M. persicae* induces senescence in *Arabidopsis*, and this is retarded (rather than promoted as in *aca10 aca12* mutants in the present work) in *phytoalexin-deficient 4* plants.[3] Our results show that *S. littoralis*, a lepidopteran that preferentially feeds on stressed leaf tissue,[34] triggers senescence and gains weight more rapidly on *aca10 aca12* leaves than on the leaves of the WT. *ACA10* and *ACA12* are potential targets for manipulation by senescence-feeders.

The adult-phase *aca10 aca12* double mutants we studied grew similarly to the WT in our short-day insect-free culture conditions. However, upon attack or in extended darkness, rosette phenotypes of the WT and double mutant diverged. Insect-attacked *aca10 aca12* double mutants displayed petiolar shrinkage and translucency on some leaves. However, this was not seen on the insect-attacked WT or on the double mutant that had been kept in the dark for 3 days. Nevertheless, both herbivore and dark treatments led to a loss of excitability and, eventually, to leaf senescence in the double mutant. We note that aphid feeding or prolonged exposure to darkness both led to a loss of excitability in *aca10 aca12* mutants without apparent tissue loss. Therefore, loss of lamina tissue is not necessary for electrical signaling failure. Our present data rather suggest a correlation between stress-induced growth arrest and loss of excitability in *aca10 aca12* mutants. We noted apparent waterlogging in the leaves of *aca10 aca12* mutants that had been maintained in prolonged darkness. A dark-induced increase in overall leaf water content has been noted previously.[35] We do not exclude the possibility that apoplastic waterlogging also occurs in insect-damaged *aca10 aca12* but may not be apparent due to water loss through damaged sites. We find that *aca10 aca12* mutants are intrinsically prone to senesce, and our biochemical analyses supported this conclusion. For example, the increased amino acid levels in *Spodoptera*-attacked double mutants appear consistent with a bulk remobilization of photosynthesis-associated proteins as has been seen when plants are exposed to prolonged carbon starvation[36]—a treatment that also induces senescence. Increased fructose levels have also been observed in senescing plants.[37] Altered fructose and amino acid homeostasis in the insect-attacked *aca10 aca12* mutants indicates a broad effect on physiology. The results illustrate an often hidden aspect of plant defense: the need to maintain physiological function during sustained stress.

Whereas leaf-to-leaf electrical signaling is jasmonate-independent,[5] anthocyanin accumulation on petioles is jasmonate-dependent.[38] The *aca10 aca12* plants did not display extensive petiole reddening after *Spodoptera* attack, suggesting that jasmonate signaling (or other factors affecting anthocyanin deposition) was decreased in the petiolar epidermis of these plants. However, in a seeming contradiction, we found higher-than-WT JA-Ile levels in the leaves of the *Spodoptera*-attacked double mutant. This may relate to senescence rather than to increased jasmonate pathway signaling. Increased levels of JA-Ile precursor jasmonic acid typify senescing *Arabidopsis* leaves.[39] Regarding defense metabolites, the levels of glucosinolates induced in response to insect attack were generally lower in the double mutant than in the WT. Together, these results distinguish *aca10 aca12* from other Ca^{2+}-related mutants, including *calmodulin-like protein 37* mutants that specifically reduce the expression of a positive regulator of the jasmonate pathway[40] and *cyclic nucleotide-gated channel 19* mutants in which both jasmonate levels and aliphatic glucosinolate levels are decreased relative to the WT.[41]

ACA10 and *ACA12* are not canonical electrical signaling genes

Clearly, due to the conditional nature of *aca10 aca12*, the two ACA proteins are not components of canonical signal pathways that underlie wound-response electrical signal generation or propagation. Instead, these gene functions are needed to maintain cell excitability and leaf defense capacity during chronic attack. During herbivore onslaught on *aca10 aca12* plants (e.g., at day 3 in the time course shown in Figure 3B), the durations of SWPs appear to decrease more quickly than the amplitudes of the electrical signal. We note that the SWP in Arabidopsis can be deconvoluted genetically into a leading spike-like depolarization followed by a long-duration depolarized phase.[7] The latter phase may be the most sensitive to perturbations in ACA10 and ACA12 function. Although *ACA10* and *ACA12* are in different clusters of the *ACA* gene family,[21] both genes are thought to encode plasma membrane-localized Ca^{2+} pumps.[42] It is therefore likely that mutation of these genes affects Ca^{2+} homeostasis. One possibility, given that we failed to generate WT-sized *aca10c aca12c* plants expressing GCaMP3, is that, in the presence of this reporter gene, deregulated Ca^{2+} levels in specific cells or subcellular environments are toxic in this mutant. The ratiometric Ca^{2+} reporter YC3.6 could, however, be expressed in the double mutant. YC3.6 output prior to wounding was lower in *aca10c aca12c* than in the WT and, in response to acute wounding, cytosolic Ca^{2+} levels remained lower in the double mutant than in the WT. Intriguingly, these results differ markedly from those of obtained with an *aca8* single mutant, which has elevated Ca^{2+} levels in resting leaves.[22] Our results also differ from those for *aca4 aca11*[23] and *aca1 aca2 aca7* mutants[19] where elicitor-induced cytosolic Ca^{2+} levels were higher than those in the WT. In summary, altered Ca^{2+} homeostasis in *aca10c aca12c* relative to the WT in response to single mechanical wounds was detected.

The role of the vasculature under sustained attack

The phloem is a site of intense, stress-induced Ca^{2+} signaling,[43] and aphid stylet ingress into the mesophyll elicits local cytosolic

(F) Electrical signaling failure in *aca10c aca12c* placed in the dark. 5-week-old plants were transferred to darkness at 12h00 (ZT = 4 h) and left in darkness for 24 h until 12h00 the following day. Plants were then transferred back to light and SWPs were measured on leaf 13, following single mechanical wounds on leaf 8. Means ± SD, n = 20–34. The inset shows WT and *aca10c aca12c* rosettes after 24 incubation in darkness. Inset scale bars, 1 cm.
See also Figure S6.

Ca^{2+} transients adjacent to the phloem.[44] *B. brassicae* is a phloem-feeder,[26] and the striking aphid-feeding-induced failure of long-distance electrical signaling in *aca10 aca12* suggested a strong impact of the mutant on this tissue. Both *ACA10* and *ACA12* transcripts are found in companion cells, where *ACA10* transcript levels exceed those of *ACA12*.[31] This led us to investigate whether the defense capacity against *S. littoralis* in the *aca10c aca12c* mutant could be rescued by expressing *ACA10* in specific vascular cell types. *ACA10* was expressed from three different promoters in the *aca10c aca12c* double mutant, and the resultant plants were then challenged with *S. littoralis*. Insects on the *aca10c aca12c* double mutant grew rapidly, but insect weight gain on $SUC2_{pro}$*:ACA10-GUS* / *aca10c aca12c* plants was similar to that on the WT. We noted that the xylem contact cell-expressed $LOX6_{pro}$*:ACA10-GUS* construct also partially rescued *aca10c aca12c* from *S. littoralis*. We interpret this to mean that both phloem and xylem excitability play an important role in plant defense. Despite damage to their leaves, the $SUC2_{pro}$*:ACA10-GUS* / *aca10c aca12c* plants still produced WT-like electrical signals when wounded. We conclude that vascular cell excitability, probably by affecting whole-leaf physiology, underlies much of the *aca10 aca12* phenotype. Outside the vasculature, the *ACA10* promoter is active in guard cells,[45] and we leave open the possibility that guard cell function is impaired in *aca10 aca12* mutants. Together, our observations were used to build a model for ACA10/ACA12 roles during herbivory (Figure S6). The model proposes that, in *aca10 aca12*, the failure of phloem cells (and, to a lesser extent, xylem contact cells) to repolarize during prolonged stress lowers overall vascular excitability. This loss of excitability then leads to a collapse of physiological functions, growth arrest, and senescence.

Summarizing, numerous genes with roles in plant-insect interactions have been identified.[13] The bulk of these genes encode direct and indirect defense functions or operate in the regulation of defense signal pathways. *ACA10* and *ACA12* act differently. We envisage that the calcium pumps encoded by these genes promote survival by maintaing cell excitability when energy is limiting. The role of these proteins in protection against both insect damage and dark-induced senescence supports this contention. That is, mutants in genes underlying cell excitability are expected to have broad functions not limited to a particular stress. Such genes may be the targets of senescence-inducing organisms. We propose that loss of excitability in key vascular cell populations (chiefly the phloem but also in xylem contact cells) underlies defense collapse and physiological dysfunction in *aca10 aca12*. These double mutants are potentially valuable tools for further studies of early events in inducible senescence.

STAR★METHODS

Detailed methods are provided in the online version of this paper and include the following:

SUPPLEMENTAL INFORMATION

Supplemental information can be found online at https://doi.org/10.1016/j.cub.2022.03.059.

ACKNOWLEDGMENTS

J. Hua (Cornell University) kindly provided several *aca* double-mutant lines, including the T-DNA insertion mutant *aca10 aca12*. We thank R. Ursache (University of Lausanne) for helpful advice and vectors for CRISPR-Cas9 experiments and M. Krebs (Heidelberg University) for YC3.6 seeds. Niko Geldner (University of Lausanne) provided access to a TAC library and gave critical comments on the manuscript. This work was funded by University of Lausanne and Swiss National Science Foundation grants (31003A-138235 and 31003A-175566) to E.E.F.

AUTHOR CONTRIBUTIONS

N.F. performed genetics, bioassays, electrophysiology, and microscopy. G.G. performed jasmonate and glucosinolate analyses. G.L. and N.F. performed calcium reporter assays. M.F.-S. performed amino acid and hexose analyses. S.S. performed GUS staining and qPCRs. N.F., G.L., E.E.F., and S.C.Z. analyzed data. E.E.F. wrote the paper.

DECLARATION OF INTERESTS

The authors declare no competing interests.

Received: August 31, 2021
Revised: February 9, 2022
Accepted: March 21, 2022
Published: April 11, 2022

REFERENCES

1. Costa, J.T., and Pierce, N.E. (1997). Social evolution in the Lepidoptera: ecological context and communication in larval societies. In The Evolution of Social Behaviour in Insects and Arachnids, J.C. Choe, and B.J. Crespi, eds. (Cambridge University Press), pp. 407–442.
2. Campbell, S.A., and Stastny, M. (2015). Benefits of gregarious feeding by aposematic caterpillars depend on group age structure. Oecologia *177*, 715–721.
3. Pegadaraju, V., Knepper, C., Reese, J., and Shah, J. (2005). Premature leaf senescence modulated by the Arabidopsis *PHYTOALEXIN*

DEFICIENT4 gene is associated with defense against the phloem-feeding green peach aphid. Plant Physiol. *139*, 1927–1934.

4. Maffei, M., Bossi, S., Spiteller, D., Mithöfer, A., and Boland, W. (2004). Effects of feeding *Spodoptera littoralis* on lima bean leaves. I. Membrane potentials, intracellular calcium variations, oral secretions, and regurgitate components. Plant Physiol. *134*, 1752–1762.
5. Mousavi, S.A., Chauvin, A., Pascaud, F., Kellenberger, S., and Farmer, E.E. (2013). Glutamate receptor-like genes mediate leaf-to-leaf wound signalling. Nature *500*, 422–426.
6. Zimmermann, M.R., Mithöfer, A., Will, T., Felle, H.H., and Furch, A.C. (2016). Herbivore-triggered electrophysiological reactions: candidates for systemic signals in higher plants and the challenge of their identification. Plant Physiol. *170*, 2407–2419.
7. Kurenda, A., Nguyen, C.-T., Chételat, A., Stolz, S., and Farmer, E.E. (2019). Insect-damaged Arabidopsis moves like wounded *Mimosa pudica*. Proc. Natl. Acad. Sci. USA *116*, 26066–26071.
8. Nguyen, C.T., Kurenda, A., Stolz, S., Chételat, A., and Farmer, E.E. (2018). Identification of cell populations necessary for leaf-to-leaf electrical signaling in a wounded plant. Proc. Natl. Acad. Sci. USA *115*, 10178–10183.
9. Yan, C., Fan, M., Yang, M., Zhao, J., Zhang, W., Su, Y., Xiao, L., Deng, H., and Xie, D. (2018). Injury activates Ca^{2+}/calmodulin-dependent phosphorylation of JAV1-JAZ8-WRKY51 complex for jasmonate biosynthesis. Mol. Cell *70*, 136–149.e7.
10. Wang, J., Wu, D., Wang, Y., and Xie, D. (2019). Jasmonate action in plant defense against insects. J. Exp. Bot. *70*, 3391–3400.
11. Wang, X., Zhu, B., Jiang, Z., and Wang, S. (2019). Calcium-mediation of jasmonate biosynthesis and signaling in plants. Plant Sci. *287*, 110192.
12. Neilson, E.H., Goodger, J.Q., Woodrow, I.E., and Møller, B.L. (2013). Plant chemical defense: at what cost? Trends Plant Sci. *18*, 250–258.
13. Erb, M., and Reymond, P. (2019). Molecular interactions between plants and insect herbivores. Annu. Rev. Plant Biol. *70*, 527–557.
14. Geisler, M., Axelsen, K.B., Harper, J.F., and Palmgren, M.G. (2000). Molecular aspects of higher plant P-type Ca^{2+}-ATPases. Biochim. Biophys. Acta *1465*, 52–78.
15. Fuglsang, A.T., and Palmgren, M. (2021). Proton and calcium pumping P-type ATPases and their regulation of plant responses to the environment. Plant Physiol. *187*, 1856–1875.
16. Demidchik, V., Shabala, S., Isayenkov, S., Cuin, T.A., and Pottosin, I. (2018). Calcium transport across plant membranes: mechanisms and functions. New Phytol. *220*, 49–69.
17. Kudla, J., Becker, D., Grill, E., Hedrich, R., Hippler, M., Kummer, U., Parniske, M., Romeis, T., and Schumacher, K. (2018). Advances and current challenges in calcium signaling. New Phytol. *218*, 414–431.
18. Boursiac, Y., Lee, S.M., Romanowsky, S., Blank, R., Sladek, C., Chung, W.S., and Harper, J.F. (2010). Disruption of the vacuolar calcium-ATPases in Arabidopsis results in the activation of a salicylic acid-dependent programmed cell death pathway. Plant Physiol. *154*, 1158–1171.
19. Rahmati Ishka, M.R., Brown, E., Rosenberg, A., Romanowsky, S., Davis, J.A., Choi, W.G., and Harper, J.F. (2021). Arabidopsis Ca^{2+}-ATPases 1, 2, and 7 in the endoplasmic reticulum contribute to growth and pollen fitness. Plant Physiol. *185*, 1966–1985.
20. Frei dit Frey, N.F., Mbengue, M., Kwaaitaal, M., Nitsch, L., Altenbach, D., Häweker, H., Lozano-Duran, R., Njo, M.F., Beeckman, T., Huettel, B., and Borst, J.W. (2012). Plasma membrane calcium ATPases are important components of receptor-mediated signaling in plant immune responses and development. Plant Physiol. *159*, 798–809.
21. Yu, H., Yan, J., Du, X., and Hua, J. (2018). Overlapping and differential roles of plasma membrane calcium ATPases in Arabidopsis growth and environmental responses. J. Exp. Bot. *69*, 2693–2703.
22. Costa, A., Luoni, L., Marrano, C.A., Hashimoto, K., Köster, P., Giacometti, S., De Michelis, M.I., Kudla, J., and Bonza, M.C. (2017). Ca^{2+}-dependent phosphoregulation of the plasma membrane Ca^{2+}-ATPase ACA8 modulates stimulus-induced calcium signatures. J. Exp. Bot. *68*, 3215–3230.
23. Hilleary, R., Paez-Valencia, J., Vens, C., Toyota, M., Palmgren, M., and Gilroy, S. (2020). Tonoplast-localized Ca^{2+} pumps regulate Ca^{2+} signals during pattern-triggered immunity in Arabidopsis thaliana. Proc. Natl. Acad. Sci. USA *117*, 18849–18857.
24. Waadt, R., Krebs, M., Kudla, J., and Schumacher, K. (2017). Multiparameter imaging of calcium and abscisic acid and high-resolution quantitative calcium measurements using R-GECO1-mTurquoise in Arabidopsis. New Phytol. *216*, 303–320.
25. Krebs, M., Held, K., Binder, A., Hashimoto, K., Den Herder, G., Parniske, M., Kudla, J., and Schumacher, K. (2012). FRET-based genetically encoded sensors allow high-resolution live cell imaging of Ca^{2+} dynamics. Plant J. *69*, 181–192.
26. Cole, R.A. (1997). Comparison of feeding behaviour of two *Brassica* pests *Brevicoryne brassicae* and *Myzus persicae* on wild and cultivated *Brassica* species. Entomol. Experim Applic. *85*, 135–143.
27. Woo, H.R., Kim, H.J., Lim, P.O., and Nam, H.G. (2019). Leaf senescence: systems and dynamics aspects. Annu. Rev. Plant Biol. *70*, 347–376.
28. Gasperini, D., Chauvin, A., Acosta, I.F., Kurenda, A., Stolz, S., Chételat, A., Wolfender, J.L., and Farmer, E.E. (2015). Axial and radial oxylipin transport. Plant Physiol. *169*, 2244–2254.
29. Truernit, E., and Sauer, N. (1995). The promoter of the *Arabidopsis thaliana SUC2* sucrose-H+ symporter gene directs expression of β-glucuronidase to the phloem: evidence for phloem loading and unloading by SUC2. Planta *196*, 564–570.
30. Kim, J.Y., Symeonidi, E., Pang, T.Y., Denyer, T., Weidauer, D., Bezrutczyk, M., Miras, M., Zöllner, N., Hartwig, T., Wudick, M.M., et al. (2021). Distinct identities of leaf phloem cells revealed by single cell transcriptomics. Plant Cell *33*, 511–530.
31. You, Y., Sawikowska, A., Lee, J.E., Benstein, R.M., Neumann, M., Krajewski, P., and Schmid, M. (2019). Phloem companion cell-specific transcriptomic and epigenomic analyses identify MRF1, a regulator of flowering. Plant Cell *31*, 325–345.
32. Liebsch, D., and Keech, O. (2016). Dark-induced leaf senescence: new insights into a complex light-dependent regulatory pathway. New Phytol. *212*, 563–570.
33. White, T.C.R. (2015). Senescence-feeders: a new trophic sub-guild of insect herbivores. J. Appl. Entomol. *139*, 11–22.
34. Gutbrodt, B., Dorn, S., Unsicker, S.B., and Mody, K. (2012). Species-specific responses of herbivores to within-plant and environmentally mediated between-plant variability in plant chemistry. Chemoecology *22*, 101–111.
35. Law, S.R., Chrobok, D., Juvany, M., Delhomme, N., Lindén, P., Brouwer, B., Ahad, A., Moritz, T., Jansson, S., Gardeström, P., and Keech, O. (2018). Darkened leaves use different metabolic strategies for senescence and survival. Plant Physiol. *177*, 132–150.
36. Usadel, B., Bläsing, O.E., Gibon, Y., Retzlaff, K., Höhne, M., Günther, M., and Stitt, M. (2008). Global transcript levels respond to small changes of the carbon status during progressive exhaustion of carbohydrates in Arabidopsis rosettes. Plant Physiol *146*, 1834–1861.
37. Wingler, A., Purdy, S., MacLean, J.A., and Pourtau, N. (2006). The role of sugars in integrating environmental signals during the regulation of leaf senescence. J. Exp. Bot. *57*, 391–399.
38. Gan, Y., Li, H., Xie, Y., Wu, W., Li, M., Wang, X., and Huang, J. (2014). THF1 mutations lead to increased basal and wound-induced levels of oxylipins that stimulate anthocyanin biosynthesis via COI1 signaling in Arabidopsis. J. Integr. Plant Biol. *56*, 916–927.
39. Seltmann, M.A., Stingl, N.E., Lautenschlaeger, J.K., Krischke, M., Mueller, M.J., and Berger, S. (2010). Differential impact of lipoxygenase 2 and jasmonates on natural and stress-induced senescence in Arabidopsis. Plant Physiol. *152*, 1940–1950.
40. Scholz, S.S., Vadassery, J., Heyer, M., Reichelt, M., Bender, K.W., Snedden, W.A., Boland, W., and Mithöfer, A. (2014). Mutation of the Arabidopsis calmodulin-like protein CML37 deregulates the jasmonate

pathway and enhances susceptibility to herbivory. Mol. Plant *7*, 1712–1726.

41. Meena, M.K., Prajapati, R., Krishna, D., Divakaran, K., Pandey, Y., Reichelt, M., Mathew, M.K., Boland, W., Mithöfer, A., and Vadassery, J. (2019). The Ca^{2+} channel CNGC19 regulates Arabidopsis defense against *Spodoptera* herbivory. Plant Cell *31*, 1539–1562.
42. García Bossi, J., Kumar, K., Barberini, M.L., Domínguez, G.D., Rondón Guerrero, Y.D.C., Marino-Buslje, C., Obertello, M., Muschietti, J.P., and Estevez, J.M. (2020). The role of P-type IIA and P-type IIB Ca^{2+}-ATPases in plant development and growth. J. Exp. Bot. *71*, 1239–1248.
43. van Bel, A.J., Furch, A.C., Will, T., Buxa, S.V., Musetti, R., and Hafke, J.B. (2014). Spread the news: systemic dissemination and local impact of Ca^{2+} signals along the phloem pathway. J. Exp. Bot. *65*, 1761–1787.
44. Vincent, T.R., Avramova, M., Canham, J., Higgins, P., Bilkey, N., Mugford, S.T., Pitino, M., Toyota, M., Gilroy, S., Miller, A.J., Hogenhout, S.A., and Sanders, D. (2017). Interplay of plasma membrane and vacuolar ion channels, together with BAK1, elicits rapid cytosolic calcium elevations in Arabidopsis during aphid feeding. Plant Cell *29*, 1460–1479.
45. Schiøtt, M., and Palmgren, M.G. (2005). Two plant Ca^{2+} pumps expressed in stomatal guard cells show opposite expression patterns during cold stress. Physiol. Plant. *124*, 278–283.
46. Glauser, G., Vallat, A., and Balmer, D. (2014). Hormone profiling. In Arabidopsis Protocols (Humana Press), pp. 597–608. https://doi.org/10.1007/978-1-62703-580-4_31.
47. Li, X., Chanroj, S., Wu, Z., Romanowsky, S.M., Harper, J.F., and Sze, H. (2008). A distinct endosomal Ca^{2+}/Mn^{2+} pump affects root growth through the secretory process. Plant Physiol. *147*, 1675–1689.
48. Jezek, M., Silva-Alvim, F.A.L., Hills, A., Donald, N., Ishka, M.R., Shadbolt, J., He, B., Lawson, T., Harper, J.F., Wang, Y., Lew, V.L., and Blatt, M.R. (2021). Guard cell endomembrane Ca^{2+}-ATPases underpin a 'carbon memory' of photosynthetic assimilation that impacts on water-use efficiency. Nat. Plants *7*, 1301–1313.
49. Iwano, M., Igarashi, M., Tarutani, Y., Kaothien-Nakayama, P., Nakayama, H., Moriyama, H., Yakabe, R., Entani, T., Shimosato-Asano, H., Ueki, M., Tamiya, G., and Takayama, S. (2014). A pollen coat–inducible autoinhibited Ca^{2+}-ATPase expressed in stigmatic papilla cells is required for compatible pollination in the Brassicaceae. Plant Cell *26*, 636–649.
50. Ursache, R., Fujita, S., Dénervaud Tendon, V., and Geldner, N. (2021). Combined fluorescent seed selection and multiplex CRISPR/Cas9 assembly for fast generation of multiple Arabidopsis mutants. Plant Methods *17*, 111.
51. Broothaerts, W., Mitchell, H.J., Weir, B., Kaines, S., Smith, L.M., Yang, W., Mayer, J.E., Roa-Rodríguez, C., and Jefferson, R.A. (2005). Gene transfer to plants by diverse species of bacteria. Nature *433*, 629–633.
52. Schneider, C.A., Rasband, W.S., and Eliceiri, K.W. (2012). NIH Image to ImageJ: 25 years of image analysis. Nat. Methods *9*, 671–675.
53. Oñate-Sánchez, L., and Vicente-Carbajosa, J. (2008). DNA-free RNA isolation protocols for Arabidopsis thaliana, including seeds and siliques. BMC Res. Notes *1*, 93.
54. Czechowski, T., Stitt, M., Altmann, T., Udvardi, M.K., and Scheible, W.R. (2005). Genome analysis genome-wide identification and testing of superior reference genes for transcript Normalizationin Arabidopsis. Plant Physiol. *139*, 5–17.
55. Livak, K.J., and Schmittgen, T.D. (2001). Analysis of relative gene expression data using real-time quantitative PCR and the 2(-delta delta C(T)) method. Methods *25*, 402–408.
56. Glauser, G., Schweizer, F., Turlings, T.C.J., and Reymond, P. (2012). Rapid profiling of intact glucosinolates in Arabidopsis Leaves by UHPLC-QTOFMS using a charged surface hybrid column. Phytochem. Anal. *23*, 520–528.
57. Zhang, X., Henriques, R., Lin, S.S., Niu, Q.W., and Chua, N.H. (2006). Agrobacterium-mediated transformation of *Arabidopsis thaliana* using the floral dip method. Nat. Protoc. *1*, 641–646.
58. Ritchie, R.J. (2006). Consistent sets of spectrophotometric chlorophyll equations for acetone, methanol and ethanol solvents. Photosynth. Res. *89*, 27–41.
59. Arrivault, S., Guenther, M., Ivakov, A., Feil, R., Vosloh, D., Van Dongen, J.T., Sulpice, R., and Stitt, M. (2009). Use of reverse-phase liquid chromatography, linked to tandem mass spectrometry, to profile the Calvin cycle and other metabolic intermediates in Arabidopsis rosettes at different carbon dioxide concentrations. Plant J. *59*, 826–839.
60. Buescher, J.M., Moco, S., Sauer, U., and Zamboni, N. (2010). Ultrahigh performance liquid chromatography-tandem mass spectrometry method for fast and robust quantification of anionic and aromatic metabolites. Anal. Chem. *82*, 4403–4412.
61. Egli, B., Kölling, K., Köhler, C., Zeeman, S.C., and Streb, S. (2010). Loss of cytosolic phosphoglucomutase compromises gametophyte development in Arabidopsis. Plant Physiol. *154*, 1659–1671.
62. Zhou, R., Benavente, L.M., Stepanova, A.N., and Alonso, J.M. (2011). A recombineering-based gene tagging system for Arabidopsis. Plant J. *66*, 712–723.

STAR★METHODS

KEY RESOURCES TABLE

REAGENT or RESOURCE	SOURCE	IDENTIFIER
Bacterial and virus strains		
Escherichia coli (Top10)	Invitrogen	404003
Agrobacterium tumefaciens (GV3101)	Widely available	N/A
Chemicals, peptides, and recombinant proteins		
ethylacetate (HPLC grade)	Fisher Chemicals	CAS 141-78-6
formic acid (p.a)	Sigma-Aldrich	CAS 64-18-6
acetic acid	Sigma-Aldrich	49199
methanol (HPLC grade)	Fisher Chemicals	CAS 67-56-1
Water (milli-Q)	Merck Millipore	N/A
acetonitrile (LC-MS grade)	Biosolve Chimie	CAS 75-05-8
formic acid (LC-MS grade)	Biosolve Chimie	CAS 64-18-6
Jasmonoyl-S-isoleucine	OlChemim	146 232
Jasmonoyl-isoleucine-$^{13}C_6$	Glauser et al.[46]	N/A
glutaraldehyde	Signa-Aldrich	G6882
formaldehyde	Applichem	131328.1211
Chloroform, CHROMASOLV Plus	Sigma-Aldrich	650471
Methanol Chromasolv, Gradient grade	Sigma-Aldrich	348851
Tributylamine	Sigma-Aldrich	90781
phosphoric acid	Fluka	79617
2-Propanol LC-MS CHROMASOLV	Sigma-Aldrich	34965
Sodium hydroxide 50%	Sigma-Aldrich	415413
sucrose	Sigma-Aldrich	84099
fructose	Sigma-Aldrich	F0127
glucose	Sigma-Aldrich	G5146
Amino Acids Mix Solution	Sigma-Aldrich	79248
L-asparagine anhydrous	Fluka	11150
L-glutamine	Fluka	49420
L-tryptophan	Fluka	93660
MS medium	Duchefa Biochimie	MO221
BASTA (phosphinotricin)	Duchefa	PO159
X-Gluc	Carbosynth LLC	B-7300
Bbs1	NEB	R3539S
Gotaq polymerase	Promega	M784B
TaKaRa 5X PrimeScript	Takara Bio	RR036A
Experimental models: Organisms/strains		
WT Col-0	widely available	N/A
eca1	Nottingham Arabidopsis Stock Center	SALK_119898
eca2	Nottingham Arabidopsis Stock Center	SALK_039146
eca3a	Li et al.[47]	SALK_045567
eca3b	Nottingham Arabidopsis Stock Center	SALK_070619
eca4	Nottingham Arabidopsis Stock Center	SALK_048468
aca 1	Nottingham Arabidopsis Stock Center	SALK_145077
aca2	Jezek et al.[48]	SALK_082624
aca4	Boursiac et al.[18]	SALK_029620
aca10	Frei dit Frey et al.[20]	GK-044H01
aca11	Boursiac et al.[18]	SAIL_269_C07

(*Continued on next page*)

Continued

REAGENT or RESOURCE	SOURCE	IDENTIFIER
aca12	Iwano et al.[49]	SALK_098383
aca13	Iwano et al.[49]	SAIL_878_B06
eca2 eca3a	This study	N/A
eca2 eca4	This study	N/A
eca3a eca4	This study	N/A
aca2 eca1	This study	N/A
aca1 eca2	This study	N/A
aca4 aca11	This study	N/A
aca8 aca10	Yu et al. [21]	N/A
aca8 aca12	Yu et al.[21]	N/A
aca8 aca13	Yu et al.[21]	N/A
aca10 aca12	Yu et al.[21]	N/A
aca12 aca13	Yu et al.[21]	N/A
aca10c aca12c	This study	N/A
$UBQ10_{pro}$:NES-YC3.6/Col-0	Krebs et al.[25]	N/A
$LOX6_{pro}$:ACA10-GUS/aca10c aca12c	This study	N/A
$SUC2_{pro}$:ACA10-GUS/aca10c aca12c	This study	N/A
$CAB3_{pro}$:ACA10-GUS/aca10c aca12c	This study	N/A
Spodoptera littoralis	Syngenta	N/A
Brevicoryne brassicae	Grown in house	N/A
Oligonucleotides		
Primers used for genotyping, see Data S1A	This study	N/A
Primers used for qRT-PCR, see Data S1B	This study	N/A
Guide RNAs used for CRISPR, see Data S1C	This study	N/A
Recombinant DNA		
pRU41-46	Ursache et al.[50]	N/A
pSF280	Ursache et al.[50]	N/A
pU3	Ursache et al.[50]	N/A
pU6	Ursache et al.[50]	N/A
pUC57	Widely available	N/A
$LOX6_{pro}$:ACA10g-GUS	This study	N/A
$SUC2_{pro}$:ACA10g-GUS	This study	N/A
$CAB3_{pro}$:ACA10g-GUS	This study	N/A
PcUBi4-2	Ursache et al.[50]	N/A
pEC1.2	Ursache et al.[50]	N/A
GUSPlus	Broothaerts et al.[51]	www.cambia.org
Software and algorithms		
Multiquant 3.0.3	Sciex	N/A
Analyst 1.5.1	Sciex	N/A
MassLynx 4.1	Waters	N/A
Chromeleon	ThermoFisher	N/A
Labscribe3	iWorx System, Inc	N/A
ImageJ 1.53k	Schneider et al.[52]	https://imagej.nih.gov/ij/
QuantStudio 3 v1.5.2.	ThermoFisher Scientific	N/A
GraphPad Prism 8	GraphPad Software, USA	https://www.graphpad.com
Other		
Dowex 1x8, 200-400 mesh	Brunschwig	20301-0025
Dowex 50WX2, 100-200 mesh	Brunschwig	20303-0025

(*Continued on next page*)

Continued

REAGENT or RESOURCE	SOURCE	IDENTIFIER
2 mm glass beads	Merck Millipore	104014
Tissue Lyser	Qiagen	TissueLyser II
Centrifuge	Sigma	1-14
Ultrasonic bath	VWR	T 490DH
Vortex Genie 2	Scientific Industries	G560E
CentriVap	Labconco	N/A
2.0 mL microcentrifuge tubes	Eppendorf	0030.120.094
0.2 mL microcentrifuge tubes	Eppendorf	0030.124.332
HPLC glass vials 12x32 mm	Interchim	JO8440
HPLC conical inserts 250 ul	Interchim	U78191
HPLC caps 9 mm silicone/PTFE	Interchim	FJ5940
Acquity UPLC BEH C18 column	Waters	186002350
Acquity UPLC CSH C18 mm column	Waters	186005297
Acquity UPLC system	Waters	N/A
Dionex RSLC Ultimate 3000 system	ThermoFisher	N/A
Mass spectrometer	Sciex	QTRAP 4000
Hybrid Q-TOF mass spectrometer	Waters	Synapt G2
Concentrator Plus	Eppendorf	N/A
AcroPrep wwPTFE membrane	Pall	8582
UHPLC Infinity 1290	Agilent	N/A
Acquity HSS T3 C18 column	Waters	186003540
Mass spectrometer	Sciex	QTRAP 5500
Freeze Dryer Alpha 2-4	Christ	N/A
ICS 5000 (HPAEC-PAD) detector	Thermofisher	N/A
Technovit resin	Kulzer	Technovit7100
Stereomicroscope	Leica	MZ16 FA
Digital microscope	Keyence	VHX-6000
Thunder microscope	Leica	DM6B
Precision balance	Mettler-Toledo	XP205

RESOURCE AVAILABILITY

Lead contact

- Further information and requests for resources and reagents should be directed to and will be fulfilled by the lead contact: Edward Farmer: edward.farmer@unil.ch.

Materials availability

- All unique/stable reagents generated in this study are available from the lead contact without restriction.

Data and code availability

- All data available in this paper will be shared by the lead contact upon request.
- This paper does not report original code.
- Any additional information required to reanalyze the data reported in this paper is available from the lead contact upon request.

EXPERIMENTAL MODEL AND SUBJECT DETAILS

Arabidopsis thaliana Columbia background was used in all experiments. Plants were grown individually in 7 cm diameter pots under fluorescent light (100 $\mu E\ s^{-1}\ m^{-2}$) with 10 h light/14 h dark (short days), 70% humidity, 22°C during the day and 18°C at night. Growth

rooms were cleaned frequently and maintained insect-free. Seeds were stratified for 2 days at 4°C after sowing. The following T-DNA insertion mutants in the Columbia background were obtained from Nottingham Arabidopsis Stock Center (NASC): *eca1* (SALK_119898), *eca2* (SALK_039146), *eca3a* (SALK_045567),[47] *eca3b* (SALK_070619), *eca4* (SALK_048468), *aca1* (SALK_145077), *aca2* (SALK_082624),[48] *aca4* (SALK_029620),[18] *aca10* (GK-044H01),[20] *aca11* (SAIL_269_C07),[18] *aca12* (SALK_098383)[49] and *aca13* (SAIL_878_B06).[49] The double mutants of *aca8 aca10*, *aca8 aca12*, *aca8 aca13*, *aca10 aca12* and *aca12 aca13* were kindly provided by Jian Hua (School of Integrative Plant Science, Plant Biology section, Cornell University, Ithaca, USA).

METHOD DETAILS

Genotyping insertion mutants

Primers used for genotyping are presented in Data S1A.

Mechanical wounding

Numbering of leaves started from the oldest leaf emerging after the cotyledons towards the youngest in rosette center.[5] 5-week-old plants were wounded mechanically by applying single crush wounds to the apical 60% of the lamina of leaf 8 with plastic forceps.

Electrophysiology

Surface potentials were recorded with silver chloride electrodes placed on the petiole of leaf 13, 10 mm from the rosette center.[8] Electrode-leaf connections were made using 10 μl of 10 mM KCl in 0.5% (w/v) agar. A reference electrode was placed in the soil.[5] Surface potential recordings were acquired at 100 Hz using LabScribe3 software (iWorx System, Inc., Dover, NH). Depolarization amplitudes and repolarization durations were analyzed as described previously.[5]

No-choice insect feeding bioassays

Spodoptera littoralis (Egyptian cotton worm) eggs were obtain from Syngenta (Stein, Aargau, Switzerland) and stored at 10°C. Eggs were placed in a 1 L beaker containing moist filter paper to maintain humidity. The beaker was covered with Parafilm (Bemis Flexible Packaging, Neenah, WI) and placed in an incubator at 28°C for 1-2 days to allow hatching. For bioassays with *S. littoralis*, 11 pots each with a single 5- to 5.5-week-old plant, were isolated in a Plexiglass box (28.5 x 19 x 19 cm) and neonate caterpillars were placed on plants. The number of larvae per plant and duration of feeding are given in the text and figure legends. Boxes were transferred to short day conditions identical to those described above. Caterpillars were allowed to feed continuously. Living larvae were then collected and weighed on a precision balance (Mettler-Toledo XP205 (DeltaRange, Greifensee, Switzerland). For screening mutants, each box was considered as one biological replicate and two replicates were used to produce data.

Aphid feeding bioassays

Cabbage aphids (*Brevicoryne brassicae*) were reared on cabbage (*Brassica oleracea* convar. *oleracea* var. *gemmifera*). 2-3 days before experiments aphids were habituated to *A. thaliana*. For this, aphids were transferred from cabbage to *A. thaliana* in a growth chamber under the short-day conditions described above. The number of aphids per plant and the duration of feeding are given in the text and figure legends. Both the infested plants and controls were kept in the Plexiglass boxes (28.5 x 19 x 19 cm) under short day conditions.

Jasmonoyl-isoleucine (JA-Ile) quantitation

Leaves were harvested and immediately flash-frozen in liquid nitrogen. After grinding in liquid nitrogen, 100 mg of frozen powder was added to 990 μL of extraction solvent: ethyl acetate:formic acid (99.5:0.5, v/v) containing 10 μL of internal standard (IS) solution: 10 ng/mL $^{13}C_6$-JA-Ile as a standard for jasmonoyl-isoleucine.[46] After vigorous vortexing of samples, 5-10 glass beads (diameter 2-3 mm; Sigma-Aldrich, Steinheim, Germany) were added to each microtube and all samples were ground using a Tissue Lyzer (Qiagen GmbH, Hilden, Germany) at a frequency of 30 Hz for 3 min at room temperature. Following centrifugation of the mixture at 14,000 g for 3 min the resulting supernatant was transferred to a 2 mL microcentrifuge tube. All solvent was completely dried using a centrifugal evaporator (Eppendorf AG, Hamburg, Germany), and the residue was re-suspended in 100 μl of 70 % MeOH. The suspension was sonicated for 30-45 s and then centrifuged at 14,000 g for 90 s. The final supernatant was transferred to a conical glass insert (250 μl) for analysis.[46]

Transcript levels in *aca* mutants and *VSP2* trnscript levels

The following *aca* mutants used in this study were previously analysed by RT-PCR and reported to be loss-of-function mutants: *aca2*,[48] *aca4*,[18] *aca8* and *aca10*,[20] *aca11*,[18] *aca12* and *aca13*.[49] Loss of function in *aca1*, *aca10c* and *aca12c* alleles was confirmed in this study using qPCR. *VSP2* transcript levels were also analysed by qPCR. Total RNA was extracted as described previously.[53] For all experiments, RNA was extracted from leaves 8-13. Total RNA (400 ng) was copied into cDNA using TaKaRa 5X PrimeScript RT Master Mix (Takara Bio, Japan) according to the manufacturer's instructions. Quantitative Real-Time PCR (qRT-PCR) was performed on cDNA with Master Mix containing 0.1 μl GoTaq polymerase (Promega, WI) and 4 μl 5X Colorless GoTaq Reaction Buffer and 0.2mM dNTPs, 2.5mM $MgCl_2$, 30 nM 6-carboxy-X-rhodamine, 0.5X SYBER Green I (Invitrogen) and 0.25μM of both forward and reverse primers in a final volume of 20μl. Primers used for each gene are described in Data S1B. qRT-PCR was performed with a

QuantStudio 3 RealTime-PCR system (ThermoFisher Scientific, Waltham, MA) under the following conditions: initial denaturation 95°C for 2 min, followed by 40 cycles denaturation at 95°C for 30 s, annealing at 60°C for 30 s, and extension at 72°C for 30 s. Four biological replicates were used in each experiment. PCR amplicon identity was confirmed by increasing temperature from 60°C to 95°C with a ramp speed of 0.1°C per s, resulting in melting curves. CT values were acquired using QuantStudio 3 version 1.5.2 (ThermoFischer). The relative expression level of genes was normalized in relation to *UBIQUITIN-CONJUGATING ENZYME* (*UBQ21*)[54] and calculated according to the $2^{-\Delta\Delta CT}$ method.[55]

Glucosinolate extraction and analysis

Fresh frozen leaf powder (100-150 mg) from expanded adult-phase leaves (leaves 8-13) was added to 0.5 mL of H_2O:methanol:formic acid (20:80:0.1). 4-8 glass beads (diameter 2-3 mm, Sigma-Aldrich) were added to each sample and ground using a TissueLyze II (Qiagen GmbH, Hilden, Germany) for 3 min at 30 Hz. Following centrifugation for 3 min at 12,000 g, 200 μL of extract was collected and placed in an HPLC vial (Thermo Fisher Scientific, Massachusetts, USA) containing a 250 μL conical insert. Glucosinolate analysis was performed by UHPLC-QTOF-MS using an Acquity UPLC coupled to a Synapt G2 QTOF mass spectrometer (Waters, Manchester, UK) as described.[56]

CRISPR-Cas9

Using the CRISPR guide RNA design tool (https://benchling.com/) three 20-nt guide RNA (gRNA) sequences were designed for *ACA10* (At4g29900) and for *ACA12* (At3g63380) and were synthesized by Microsynth AG (Balgach, Switzerland). Following published methods[50] these gRNA sequences were separately cloned into six primary entry vectors (pRU41-46) containing the promoters *pU3* or *pU6*.[50] The gRNA sequences used are shown in Data S1C in lowercase whereas the overhangs (ATTG, GTCA and AAAC) containing restriction site of *BbsI* enzyme are shown in uppercase. Next, the six cloned gRNAs were assembled into an intermediate vector (pSF280)[50] using Goldengate cloning. Finally, two destination vectors expressing Cas-9 (pUBi4.2 and pEC1.2) were deployed to assemble all six gRNAs, with their independent promoters, within the two final constructs. The resulting clones were sequence-verified (Microsynth AG). Transgenic plants were generated by co-transformation of both sequence-verified constructs using the floral dipping method.[57] Transgenics were screened in T1 based on green seed coat fluorescence using a MZ16 FA microscope (Leica, Wetzlar, Germany). Homozygous or heterozygous lines for both *ACA10* and *ACA12* were selected using PCR and confirmed by sequencing (Microsynth AG, Balgach, Switzerland). In T2, to remove Cas-9, non-fluorescent seeds were selected. The mutations in the double mutant *aca10c aca12c* were characterized by sequencing.

Dark treatments

Plants were placed in darkness at 70% humidity, 22°C during the day and 18°C at night.

Ca^{2+} reporters

WT plants expressing GCaMP3[8] were crossed with *aca10c aca12c*. However, all double mutants expressing GCaMP3 were severely dwarfed. We therefore used an $UBQ10_{pro}$*:NES-YC3.6* variant.[25] This reporter was crossed into *aca10c aca12c* and used for ratiometric analysis of cytosolic Ca^{2+} levels. Data were collected by using a SMZ18 stereomicroscope (Nikon, Egg, Switzerland) equipped with a 0.5 X objective (NA = 0.095, SHR PLAN APO, Nikon, Egg, Switzerland), a W-VIEW GEMINI image splitting optics A12801-01 an ORCA-Flash4.0 (C11440) camera (both from Hamamatsu, Solothurn, Switzerland). Filters were from AHF Analysentechnik (Tübingen, Germany) and were mounted as following: F37-483, F37-542, F38-509 on the W-VIEW GEMINI, F39-438, F38-458, F76-460 on the microscope. The light source was provided by a SOLA SM II (Lumencor, Beaverton, OR). Fluorescence was monitored by wounding leaf 8 and acquiring fluorescent data from leaf 13 of 5-week-old plants. The ROI was defined as an area 1 mm x 1 mm (58 pixels x 58 pixels). ROIs were centred on the primary vein at the petiole/lamina junction or on the basal third of the lamina. FRET ratios were monitored at a frequency of 1 Hz. Change in fluorescence over time was analysed as FRET/CFP by using the Fiji plug-in Time Series Analyzer v2 (University of California, Los Angeles, CA). Statistical analysis was performed with Excel (Amsterdam, Netherlands) and GraphPad Prism 8 (GraphPad Software, San Diego, CA).

Plant tissue loss and phenotype analyses

Neonate *S. littoralis* larvae were allowed to feed on 5-week-old plants (4-larvae per plant). Petiole shrinkage: Each day individual plants (WT and *aca10c aca12c*) were inspected for signs of shrinkage to petioles on leaves 6 - 10. This was performed with plants still in soil and prior to fresh weight estimations. The widths of visibly affected petioles were measured using a VHX6000 microscope (Keyence, Mechelen, Belgium). The basipetal three quarters of the petioles were inspected. The ratio of the thickest part of the petiole over the thinnest part of the petiole was estimated. Each time this ratio exceeded 1.4 the petiole was scored as showing shrinkage. In no cases did we observe petiole shrinkage in healthy or damaged WT plants or in undamaged *aca10 aca12* or *aca10c aca12c* mutants grown in insect-free conditions. Fresh weight analyses: rosettes were cut off at soil level and weighed. The cut rosette was then photographed immediately for analysis with ImageJ[52] (https://imagej.nih.gov/ij/). In badly damaged plants, leaves often curl. Each of these leaves was cut off and flattened prior to photography. From these images, a total rosette outline for each plant was produced. Then, damaged regions were encircled and their areas estimated for each rosette. Note that for badly damaged plants the original leaf outline was estimated from remaining tissue. Therefore, imaging was stopped prior to complete destruction of laminae.

Chlorophyll content measurement

Samples consisted of 3 – 4 expanded leaves (from leaves 8 – 13) per plant. Leaves that were completely senescent were not harvested. After weighing leaves on a precision balance (Mettler- Toledo XP205 DeltaRang-Greifensee, Switzerland), chlorophyll (Chl) was extracted overnight in the dark at 4°C with 5 mL 90% (v/v) acetone in water. Spectrophotometry for Chl a and Chl b (at 647 nm and 664 nm wavelengths respectively) and quantitation was as described.[58] Values were normalized to fresh weight.

Sugar and amino acid analyses

For sugar and amino acid measurements, expanded adult-phase leaves (leaves 8 – 13) of 5-week-old plants were used. The samples were extracted[59] and the powdered samples (approx. 20 mg) were extracted in ice-cold chloroform : methanol 3:7 (v/v). The aqueous phase was collected and dried down in a speed vac. The samples were then resuspended in water and filtered with AcroprepAdv 350ul 0.2um WWPTFE (Pall Corporation, Vienna, Austria). Amino acids were separated by UHPLC (Agilent 1290 Infinity, Agilent Technologies, USA) with an Acquity HSS T3 C18 end-capped reverse phase column (100 Å pore size, 1.8 μm particle size, 2.1×150 mm; Waters Corp., USA) coupled to a QTRAP 5500 triple quadrupole MS (AB Sciex). Ion-pair reversed-phase chromatography[60] used eluents and gradients described in Data S1D. Eluted compounds were automatically quantified against standard curves of pure compounds using the software Multiquant (AB Sciex, Switzerland). Cysteine was measured as cystine equivalents (the oxidation product of two molecules of cysteine). The cysteine concentration was calculated two times the cystine concentration. From the same filtrates, sugars were measured.[61] The samples were applied to sequential 1.5 mL columns of Dowex-50W and Dowex-1 (Sigma-Aldrich). Neutral compounds were eluted with 5 mL of water, lyophilized, and dissolved in 100 μl of water. Sugars were separated by anion exchange chromatography (CarboPac PA-20 column) and detected with pulsed amperometric detection (HPAEC-PAD, Thermo Fisher Scientific). The eluents and gradients are described in Data S1E. Peaks were quantified using Chromeleon software (Thermo Fisher Scientific) against standard curves of pure compounds and normalized to the internal standard.

Complementation of *aca10c aca12c*

The promoters of *SUC2*, *LOX6* and *CAB3* were used to drive the expression of *ACA10-GUS* translational fusions in the *aca10c aca12c* background. The *ACA10* full length gene was amplified from the JAtY TAC-based *Arabidopsis* genomic DNA library[62] with primers containing full Gateway recombination sites using InFusion kits (Takara Bio, Mountain View, CA). *ACA10* coding region primers: forward I 5′- ACAAAAAAGCAGGCTactagtTAAGCATTTAGTTTGATTGATGTAGTAATTTGTCATTTTTTAAAGTAC-3′, reverse I 5′- GTCTTCCCTCCAATAAACTGTGGGCCTCCCTG- 3′. The amplified genomic coding region of *ACA10* was recombined using Gateway cloning to make a pDONR/221- L1-gACA10-L2 Entry clone. The *SUC2*, *LOX6* and *CAB3* promoters (> 3 kb) were then amplified from WT *A. thaliana* (Col) genomic DNA. *SUC2* promoter primers: Forward 5′- CGGGGTACCCTGCTAAAACTATT CCATTTCAAAATG -3′; Reverse 5′-TTCCCCCCCGGGATTTGACAAACCAAGAAAGTAAG- 3′. *LOX6* promoter primers: Forward 5′- CGGGGTACCGGTTGTTGAAATTTCTGATGCT -3′; Reverse 5′- TTCCCCCCCGGGTTTTGTTTGGAGTTTGGCAGT - 3′. *CAB3* promoter primers: Forward (5′-GGCATCAGAAGTCCTTGGAAGC-3′; Reverse 5′-TGAAACTTTTTGTGTTTTTTTTTTTTTTTGGTGAC-3′. *SUC2*, *LOX6* and *CAB3* promoter regions were inserted into pUC57-L4-Kpn1/Xma1-R1 and were recombined with pEN-L1-GUS Plus-L2. GUSPlus[47] was amplified without the secretion signal from pCAMBIA 1305.2 (www.cambia.org). pUC57-L4-Kpn1-*SUC2*-, -*LOX6*- and -*CAB3* -Xma1-R1, pDONR/221-L1-ACA10g-L2 and pEN-R2-GUS-L3, were sub-cloned into the destination vector pB7m34GW to generate desired fusions (*SUC2*$_{pro}$*: ACA10g-GUS*, *LOX6*$_{pro}$*: ACA10g-GUS*, and *CAB3*$_{pro}$*: ACA10g-GUS*) by Triple Gateway cloning using LR reactions. All constructs were introduced into the *aca10c aca12c* background by *Agrobacterium*-mediated flora dip transformation.[55] Transgenic plants were screened on half-strength MS medium (Duchefa Biochemie, Haarlem, Netherlands) with 40 μg/ml BASTA (PlantMedia, Dublin, OH).

GUS staining

Primary veins from leaf 8 of *ACA10-GUS* expressing plants were extracted[8] and immediately prefixed in 90% acetone on ice for 1 h. Veins were washed 2 times for 5 min with 50 mM sodium phosphate buffer (pH 7.2) then stained in 10 mM Na_2EDTA, 1 mM $K_4Fe(CN)_6$, 1 mM $K_3Fe(CN)_6$, 0.1% (v/v) Triton X-100, 0.5 mg ml^{-1} X- Gluc; 50 mM sodium phosphate buffer pH 7.2 in the dark at 37°C. Images of veins were taken with VHX-6000 digital microscope (Keyence, Mechelen, Belgium). Transversal petiole sections from *ACA10-GUS* plants were prepared as follows: 1 cm petiole sections from leaf 8 were fixed and infiltrated with GUS stain using the above procedure. Stained petiole sections were then washed for 2 times for 5 min with 50 mM sodium phosphate buffer. X-Gluc-stained petioles were fixed in glutaraldehyde/formaldehyde/50 mM sodium phosphate (pH7.2) 2:5:43 (v/v/v) for 30 min then dehydrated in an ethanol gradient (10%, 30%, 50%, 70%, 90% and twice absolute ethanol, for 30 min at each ethanol concentration). Dehydrated petioles were embedded in Technovit 7100 resin (Haslab GmbH, Ostermundigen, Switzerland) according to the manufacturer's instructions. Transversal sections of the petiole (3 μm thick) were made on a RM2255 microtome (Leica, Wetzlar, Germany). The sections were mounted in 40% (v/v) glycerol and photographed with a Thunder DM6B microscope (Leica, Wetzlar, Germany).

QUANTIFICATION AND STATISTICAL ANALYSIS

Statistical significance in pair-wise comparisons was evaluated by Student's t test (t-test). For multiple comparisons, analysis of variance (ANOVA) followed by Tukey's HSD test, were performed by GraphPad Prism 8 software (GraphPad software Inc., San Diego, CA); $P<0.05$ or less.